JOURNAL OF OPTOELECTRONICS AND ADVANCED MATERIALS Vol. 9, No. 10, October 2007, p. 3293 - 3296

Theoretical approach regarding nanometrology of the metal nanoclusters used in heterogeneous catalysis by powder x-ray diffraction method

N. ALDEA[a*], B. BARZ[b], S. PINTEA[a], F. MATEI[c]
[a]*National Institute for Research and Development of Isotopic and Molecular Technologies, P.O. Box 700 Cluj-Napoca 5, Romania*
[b]*University of Missouri Columbia, 223 Physics Building, MO 65211, USA*
[c]*University of Agricultural Sciences and Veterinary Medicine, Cluj-Napoca, Department of Mathematics and Computer Science, Calea Manastur 3-5, Romania*

In this paper we discuss a new theoretical approach for determining the metal nanocrystallite size, lattice strain and total probability of faults from the X-ray diffraction line profile broadening. The emphasis is made on the rigorous analysis of the line profiles in terms of Fourier transform. The generalized Fermi distribution function is used for the single X-ray line profile approximation in order to determine the crystallite size and the lattice strain by the deconvolution technique. Our method is implemented in a computer package program developed with Maple 10 software. We apply our method to elaborate the global structure of Au/SiO_2 nanoclusters with catalytic applications.

(Received July 3, 2007; accepted October 1, 2007)

Keywords: X-ray diffraction, gold nanoclusters, crystallite size, microstrain, stacking fault probability

1. Introduction

X-ray diffraction line profile analysis is a versatile nondestructive method that can be used in obtaining structural information (averaged over a moderately large volume of about 1 mm^3) about the metal nanoclusters with catalytic properties used in oxidation, reduction, isotopic exchange and hydrogenation reactions. From the position and the broadening of the X-ray line profile (XRLP) structural information can be obtained about the imperfect crystallite, regarding the effective crystallite size, as well as about the microstrain through the lattice deformation. Detailed theoretical aspects of the mosaic structure model are presented. In this model atoms are arranged in blocks, each block itself being an ideal crystal, but adjacent blocks are not accurately fitted together [1-7]. In this paper we describe the main parts of the computer program called SIZE.MWS written in Maple 10 language. The test run is dedicated to the global structure elaboration of the Au/SiO_2 nanoclusters.

2. Program description

The SIZE program consists of the main program body and several procedures designed to perform basic tasks as described below.

2.1. Main program

This is effectively a program that first determines the background of the X-ray line profile (XRLP) and the generalized Fermi function (GFF) parameters. These parameters are obtained by global approximation of the background and minimization of the GFF by Levenberg-Marquard algorithm [8]. The background and GFF are given by the following relations

$$B(s) = a_0 + a_1 s + a_2 s^2 + a_3 s^3, \qquad (1)$$

$$h(s) = \frac{A}{e^{a(s-c)} + e^{-b(s-c)}} \qquad (2)$$

where the s variable can be 2θ or $\frac{2\sin\theta}{\lambda}$. The values A and c describe the amplitude and position of the XRLP; a and b control its shape.

Additionally, the main program determines the particle distribution data used for calculating the average particle size given by the relations

$$\overline{D} = \int_{L_{\min}}^{L_{\max}} LP(L)\,dL, \qquad D_{\perp} = \left(\int_{L_{nim}}^{L_{\max}} \frac{P(L)}{L}\,dL \right)^{-1}, \qquad (3)$$

where $\overline{D}$ is the volumetric mean particle size and $D_{\perp}$ is the harmonic average of the thickness of the particle normal to the *(hkl)* reflecting plane [2,4]. The particle size distribution function *P(L)* is calculated as the second derivative of the strain-corrected by the Fourier transform of the true sample, and it is normalized such that its integral is equal to 1. The physical meaning of the true sample function is described in the papers [4-6]. The stacking fault probability $1.5\alpha + \beta$ (α - the sequence

fault probability, β - the twin fault probability) is given by the relation

$$\frac{1}{D_{eff}} = \frac{1}{\overline{D}} + (1.5\alpha + \beta)\frac{V_{hkl}}{a} \tag{4}$$

where V_{hkl} are the coefficients which are computed for the fcc lattice [1], D_{eff} is computed in eq. (10) and a is the lattice cell. Finally, the main program determines the crystallite size, without taking into account the lattice microstrain, using the classical Scherrer model based on the relation

$$D_{Sch} = \frac{\lambda}{4\cos\theta_0 \arcsin\left[\dfrac{\delta_f^{(s)}\lambda}{4\cos\theta_0}\right]}, \tag{5}$$

where θ_0 and $\delta_f^{(s)}$ are the gravity center and the integral width of the true sample function. The main program also calls the procedures in sequential or selective mode depending on the user's needs. The analytical and numerical processing results are displayed continuously trough a graphical user interface.

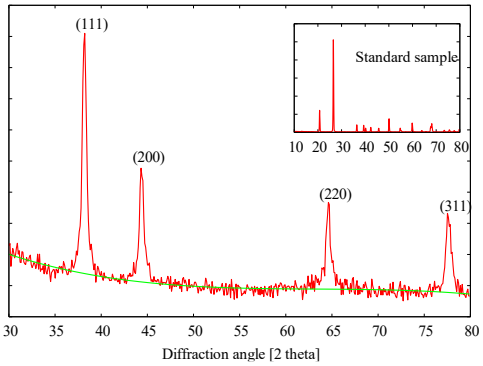

Fig. 1.The relative intensity of the (111), (200), (220) and (311) K_α experimental line profiles of Au/SiO_2 (red line) and standard sample as instrumental function SiO_2 powder (inset); background correction (green line)

2.2. Procedures f_freq and f_module

These procedures calculate the magnitude of the Fourier transform of the true sample function that has the following form

$$|F(L)| = \frac{A_h\rho_g}{A_g\rho_h}\sqrt{\frac{\cos^2\alpha + \sinh^2\beta L}{\cos^2\gamma + \sinh^2\delta L}}, \tag{6}$$

where the arguments of trigonometric and hyperbolic functions are expressed by following relationships

$$\rho = \frac{a+b}{2},\ q = \frac{a-b}{2},\ \alpha = \frac{\pi q_g}{2\rho_g},\qquad \beta = \frac{\pi^2}{\rho_g},$$

$$\gamma = \frac{\pi q_h}{2\rho_h},\ \delta = \frac{\pi^2}{\rho_h}.$$ The subscripts g and h refer to the instrumental and experimental XRLP.

2.3. Procedure f_s

This procedure determines the analytical relation of the true sample function. It is calculated by Fourier transform procedure and its form is given by the relation

$$f(s) = \frac{2A_h\rho_g}{\pi A_g}\frac{\cos\dfrac{\pi\rho_h}{2\rho_g}\cosh\rho_h s}{\cos\dfrac{\pi\rho_h}{\rho_g} + \cosh 2\rho_h s}. \tag{7}$$

2.4. Procedure int_width

Integral widths for the experimental XRLP as well as for the true sample are calculated by relations

$$\delta_h(a,b) = \frac{\pi}{(a^a b^b)^{1/(a+b)}\cos\left(\dfrac{\pi}{2}\dfrac{a-b}{a+b}\right)},$$

$$\delta_f(\rho_h,\rho_g) = \frac{\pi}{2\rho_h\cos\dfrac{\pi\rho_h}{2\rho_g}}\left(\cos\frac{\pi\rho_h}{\rho_g}+1\right). \tag{8}$$

2.5. Procedures mu_0, mu_1 and mu_2

These procedures compute the first three moments of XRLP. The first one gives the area, the second one the center of gravity and the third one the abscises of XRLP inflection [8]. They are determined by the relations

$$\mu_0 = \frac{\pi A}{2\rho\cos\dfrac{\pi q}{2\rho}},\quad \mu_1 = \frac{\pi}{2\rho}\tan\frac{\pi q}{2\rho},\quad \mu_2 = \left(\frac{\pi}{2\rho}\right)^2\left(\frac{1}{\cos^2\dfrac{\pi q}{2\rho}} + \tan^2\frac{\pi q}{2\rho}\right). \tag{9}$$

2.6. Procedures alpha_par, beta_par, gamma_par, a_par, b_par, c_par and d_par

These procedures are based on the least squares method and they are used for determining the global structural parameters in the small crystallites (L → 0) approximation. Their relations are given by

$$F(L) = 1 - L/D_{eff} - C^2 <\varepsilon^2(L)>_{hkl} L^2 + C^2 <\varepsilon^2(L)>_{hkl} L^3/D_{eff},$$
$$F(L) = a_0 + a_1 L + a_2 L^2. \tag{10}$$

2.7 Procedures beta_gen and gamma_gen

Based on the least square method these procedures determine the crystallite size and the microstrain from the general relation

$$F(L) = e^{-\left(\frac{|L|}{D_{eff}(hkl)} + \frac{2\pi^2 \left\langle \varepsilon_L^2 \right\rangle_{hkl} h_0^2 L^2}{a^2}\right)}, \qquad (11)$$

where $h^2_0=h^2+h^2+l^2$ and a is the lattice constant.

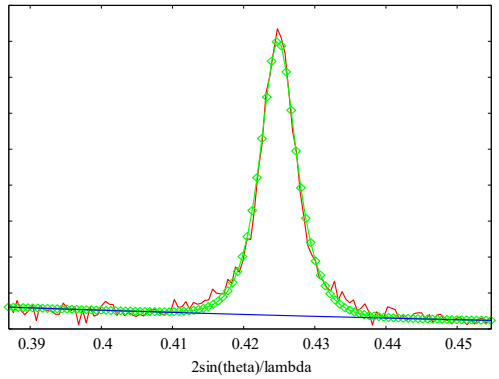

Fig. 2 The relative intensity of the (111) XRLP (red line); background correction (blue line), GFF approximation (green line+points).

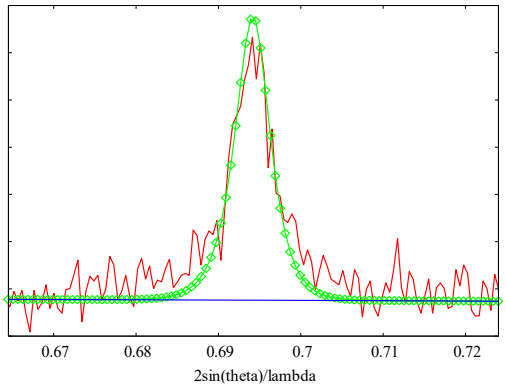

Fig.3. The relative intensity of the (220) XRLP (red line); background correction (blue line), GFF approximation (green line+points)

3. Results and discussion

Practically, it is not easy to obtain accurate values of the crystallite size and microstrain without extreme care in the experimental measurements and analysis of the XRD data. The XRLP Fourier analysis validity depends strongly on the magnitude and nature of the error propagated in the data analysis [9]. In order to minimize the propagation of these systematic errors a global approximation of the XRLP is adopted instead of the classical discrete Fourier analysis. Therefore, herein, the analysis of the diffraction line broadening in X-ray powder pattern was analytically calculated based on procedures described in the previous section using the possibilities offered by the generalized Fermi function (GFF) [10].

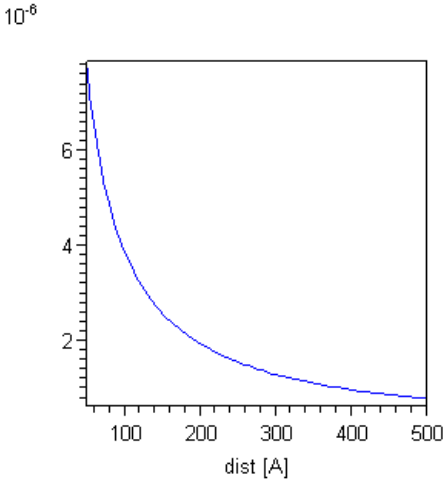

Fig. 5.Microstrain distribution function

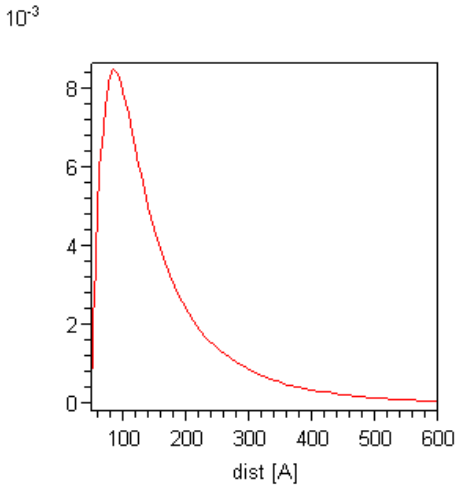

Fig. 6. Particle size distribution function.

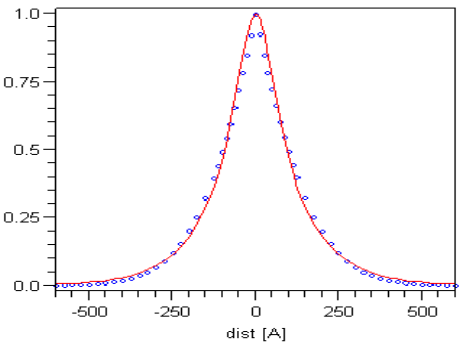

Fig. 7. Fourier transform of true samples (220) for Au/SiO_2 (red line); the theoretical Fourier transform – Eq.(11) (blue points).

In this paper we analysed the (111), (200), (220) and (311) XRLP. Their relative intensities for Au/SiO_2 investigated sample as well as for the standard SiO_2 powder sample

with respect to the diffraction angle and the background correction are presented in Fig 1. Figs. 2 and 3 show the experimental XRLPs and their approximations using GFF distributions. In all cases the curves exhibit good similarities. Table 1 contains the best-fit values and their uncertainties for the background correction and the GFF distributions. Figs. 5 and 6 describe the microstrain distribution as well as the particle size distribution corresponding to (220) XRLP. Figure 7 shows the calculated Fourier transform of the true sample function using GFF distributions for the experimental and instrumental functions and fitted by relation (11).

Table 1 Parameters of the XRLP approximated by GFF distributions.

Background correction: a_0=924.97±36.48, a_1=-34.54±2.19, a_2=0.54225±0.04186, a_3=-0.00285±0.00026				
XRLP	A	a	b	c
Standard sample	53455±67	1115.21±28.83	848.125±27.99	$0.29924\pm0.435\times10^{-6}$
(111)	1529±18.29	450±14.25	432±16.79	0.42485+0.00021
(200)	682.975±14.46	485.816±17.25	333.235±10.18	0.49±0.0012
(220)	600±26.5	500±50.44	550±88.57	0.69431±0.00037
(311)	595±24.13	525±42.09	552±80.15	0.81436±0.00033

The main numerical results of the test run for (220) XRLP are given below.

Integral width of the experimental XRLP	0.005994 $Å^{-1}$
Integral width of the true sample function	0.003994 $Å^{-1}$
Zero order moment of true sample function	1.8
Gravity center of the true sample	-0.0002242 $Å^{-1}$
Standard deviations of the true sample	-0.003233, 0.00278 $Å^{-1}$
Volumetric mean particle size	157 Å
Harmonic average of particle size	137 Å
Stacking fault probability	1.2 %
Effective crystallite size (cubic approximation)	202 Å
Microstrain parameter (cubic approximation)	0.6778×10^{-5}
Effective crystallite size (general relation)	162 Å
Microstrain parameter (general relation)	0.11×10^{-4}
Crystallite size (Scherrer method)	250 Å

4. Conclusions

In the present paper we presented a computer code capable to analyze an X-ray line profile obtained by XRD. The code was applied for the global structure determination of the gold nanoclusters supported on silicon oxide with catalytic applications in reactions such as: reduction, oxidation, hydrogenation and isotopic exchange between hydrogen and deuterium. The conclusions that can be draw from this theoretical and numerical study are:

(i) For XRLP analysis the global approximation by GFF distribution is applied instead of a numerical Fourier analysis. This can minimize the systematic errors that appear in the traditional Fourier analysis;

(ii) A variety of approximate forms of the Fourier transform are presented. Some of them are valid only for small crystallite size (D_{eff} around 100 Å) such as the parabolic approximation, while general forms can be used for any value of the variable *L*;

(iii) The SIZE package program has implemented all the methods described in the second section and it has a user's friendly interface.

References

[1] B. E. Warren, X-Ray Diffraction, Addison-Wesley Publishing Company, 1969.
[2] N. Aldea, E. Indrea, Comput. Phys. Commun **60**, 155 (1990).
[3] N. Aldea, R. Zapotinschi, C. Cosma, Fresenius J. Anal. Chem. **355**, 367 (1995).
[4] N. Aldea, A. Gluhoi, P. Marginean, C. Cosma, X. Yaning, Spectrochim. Acta Part B **55**, 997 (2000).
[5] N. Aldea, A. Gluhoi, P. Marginean, C. Cosma, Xie Yaning, H. Tiandou, W. Wu, B. Dong, Spectrochim. Acta Part B **57**, 1453 (2002).
[6] N. Aldea, C. V. Tiusan, B. Barz, J. Optoelectron. Adv. Mater. **6**(1), 225 (2004).
[7] J. Mittemeijer, P. Scardi, Diffraction Analysis of the Microstructure of materials, Springer Verlag, Berlin, Heidelberg 2004.
[8] N. Aldea, F. Aldea, Analysis techniques of physical and chemical signals, Risoprint Cluj-Napoca 2001 (in Romanian language)
[9] R. A. Young, R. J. Gerdes, A. J. C. Wilson, Acta Cryst. **22,** 155 (1967).
[10] N. Aldea, B. Barz, A. C. Gluhoi, P. Marginean X. Yaning H. Tiandou L. Tao, Z. Wu, Z. Wu, J. Optoelectron. Adv. Mater**. 6**(4), 1287 (2004).

* Corresponding author: naldea@itim-cj.ro

JOURNAL OF OPTOELECTRONICS AND ADVANCED MATERIALS Vol. 9, No. 10, October 2007, p. 3293 - 3296